Research Square

Preprints are preliminary reports that have not undergone peer review.
They should not be considered conclusive, used to inform clinical practice,
or referenced by the media as validated information.

Utilizing network pharmacology and experimental validation to investigate the underlying mechanism of Sophora davidii resists aging

Bin Deng
Guizhou University of Traditional Chinese Medicine
Zhigang Ju
Guizhou University of Traditional Chinese Medicine
Chenggang Hu
Guizhou University of Traditional Chinese Medicine
Angxin Song
Guizhou University of Traditional Chinese Medicine
Shuai Liu
Guizhou University of Traditional Chinese Medicine
Zongren Xu
Guizhou University of Traditional Chinese Medicine
Yingyi Yu
572962400@qq.com
Guizhou University of Traditional Chinese Medicine

Article

Keywords: Sophora davidii, umbilical vein endothelial cells, aging, network pharmacology, TP53-PI3K/AKT pathway

Posted Date: July 9th, 2026

DOI: https://doi.org/10.21203/rs.3.rs-9720416/v1

License: This work is licensed under a Creative Commons Attribution 4.0 International License.
Read Full License

Additional Declarations: No competing interests reported.

Abstract

Background

The Sophora davidii flower (SDF) is an important traditional Chinese medicine in Guizhou, and it has the effect of anti-aging. However, the specific mechanism of its action remains unclear. We investigated the therapeutic effects and mechanisms of SDF on anti-aging using network pharmacology and cell experiments.

Methods

The database was used to predict anti-aging-related targets of SDF, and 81 SDF-intersecting targets for aging treatment were identified. A PPI network was developed to identify key targets using degree values. Key targets were analyzed using KEGG pathway enrichment and GO function to identify pathways related to matrine's anti-aging effects. Moreover, perform molecular docking on matrine and key targets. An aging model of HUVECs was developed using the H_2O_2 induction, followed by treatment with varying concentrations of SDFE (0.5, 1 and 2 mg/mL). β-galactosidase staining assessed the positive rate of aging HUVECs, while the tube formation assay evaluated their tube formation capability. Western blot analysis was employed to detect marker proteins in the aging signaling pathway.

Results

The β-galactosidase staining demonstrated that SDFE could inhibit the senescence of HUVECs, while the tube formation assay proved that SDFE can enhance the tube forming ability. The Western blot confirmed the p53, p-Akt/Akt and p-PI3K/PI3K levels decreased significantly in all SDFE dose groups compared to the control group, exhibiting a dose-dependent pattern.

Conclusion

The results indicated that SDF could inhibit HUVEC aging, and the mechanism involved the regu-lation of the TP53-PI3K/AKT pathway.

Introduction

As global population aging intensifies, aging and associated diseases like cardiovascular diseases, osteoporosis, diabetes, and neurodegenerative disorders have emerged as significant public health challenges[1]. Aging is characterized not only by the gradual decline in physiological functions but also as a critical risk factor for various chronic diseases[2]. Key features of aging include alterations in gene expression, reduced cellular function, and tissue structure degeneration[3]. A decline in cell function

characterizes aging. As an important component of the vascular wall, endothelial cell dysfunction is closely related to the aging process[4]. Therefore, exploring effective strategies to prevent vascular endothelial cell aging is of great significance for delaying the aging process.

Traditional Chinese medicine and its active ingredients have shown great potential in anti-aging research due to their multi-target and multi-pathway regulatory effects[5]. The flower of Sophora davidii (SDF, depicted in Fig. 1.A) are plentiful in the Guizhou regions of China. This wild vegetable is highly nutritious and can be prepared into a variety of delicious dishes (Fig. 1.B). Traditionally, it is known for detoxifying, cooling blood, clearing heat, sore throat and lung heat cough[6,7]. SDF are rich in flavonoids and alkaloids, demonstrating strong anti-inflammatory and antimicrobial properties[8]. In addition, the main components of the white thorn flower, such as matrine, also play a significant role in delaying the onset of age-related diseases. Some studies have reported that matrine can prevent Alzheimer's disease[9], and protect mice from D-galactose-induced aging[10]. However, the potential anti-aging mechanism of the white thorn flower remains unclear and warrants further research. This study employs network pharmacology and cellular validation to explore the anti-aging effects of white prickle flower extract on human umbilical vein endothelial cells (HUVECs). The aim is to provide a scientific basis for using SDF in anti-aging applications.

Methods

Preparation of SDFE samples

The specimen of SDF was collected by the Herbarium of Guizhou University of Traditional Chinese Medicine, and the specimen number is GZTM0094560. We obtained the permission to collect from Guizhou University of Traditional Chinese Medicine.The SDF (500 g) was collected from the experimental field of Guizhou University of Traditional Chinese Medicine, and was identified by Liu Shuai. Experimental research and field studies on SDF, including the collection of the plant material are in compliance with relevant institutional, national, and international guidelines and legislation. The SDF (500 g) were refluxed for 2 h. Then, the extract was filtered, and the residue was further refluxed with 50% ethanol for 2 h. Finally, the filtrate was concentrated by a rotary evaporator and freeze-dried to obtain SDFE powder, which was stored at -16°C.

Acquisition of target points for SDF

The primary components and their target sites of SDF were identified using the following databases: SwissTargetPrediction, TCSMP, BATMAN-TCM, PharmMapper, SuperPred and TargetNet. The UniProt by filtering for “Human” Standardize the target points, then merge and eliminate duplicates from all targets to obtain the final target points for SDF.

Retrieval of Aging-related targets

Aging-related targets were identified using the search term “aging” from the following databases: GeneCards, TTD, PharmGKB, OMIM, and CTD. Then, targets standardized by UniProt, and duplicates were eliminated to obtain the final action targets for aging. At the same time, aging-related targets were identified using the GEO2R in NCBI GEO database. Targets were chosen based on $p < 0.05$, followed by the generation of a volcano plot.

Intersection targets of SDF and aging

Utilize the online tool “Venn Diagram” to create Venn diagrams. We identified the intersection targets between SDF and aging.

Construction of PPI Network and Selection of Core Targets

The PPI network was constructed using the STRING13 database. The “Multiple Proteins” option was chosen, and intersection targets were entered. “Homo sapiens” was designated as the “Organism”, The PPI network was then visually analyzed with Cyto-scape 3.8.2. In Cytoscape, Network Analyzer was used to calculate degree values in the PPI network.

GO and KEGG Analysis

Refer to the research literature of Kanehisa’s laboratory[11,12], intersected gene targets were input using the species “H. sapiens” on the Metascape. A specialized analysis was performed for KEGG pathway and GO. The top 30 GO terms were selected and visualized. KEGG pathway analysis results were compiled, and gener-ated a bubble chart.

Construction of Protein-GO-KEGG Network

The protein-GO-KEGG network was built in Cytoscape 3.8.2. Metascape identified the top 10 KEGG and GO entries with the lowest *p*-values, and the corresponding proteins were compiled into Excel files. The files were imported into Cytoscape for visualization.

Molecular docking

The 3D structures of the core target protein in the PPI network were obtained from PDB. While the 3D models of the top 5 active ingredients in the compound-target network were retrieved from the NCBI PubChem database. AutoDock Vina was utilized for molec-ular docking to evaluate the binding energies between the compounds and their targets. PyMOL software was utilized once more for visualizing the docking results.

Cell culture

HUVECs are sourced from the ATCC (USA, #AC337632). HUVECs were cultured in DMEM (Gibco, USA, #11965092) supplemented with 10% fetal bovine serum at 37°C in a 5% CO_2 incubator. HUVECs were seeded in 60 mm culture dishes (4×10^5 cells/dish) and incubated for 24 hours to allow attachment. Subsequently, 0.2 mmol/L H_2O_2 (Sigma, USA, #18304) was added for 24 h to induce aging damage[13]. Different concentrations of SDFE—control (0 mg/mL), low (0.5 mg/mL), medium (1 mg/mL), and high (2 mg/mL)—were then administered for another 24 h.

β-galactosidase staining

HUVECs were washed twice with PBS (Sigma, USA, #P3813) and fixed at room tem-perature using 4% paraformaldehyde (Sigma, USA, #441244) for 15 min. Following fixative aspiration, the cells underwent three 3-minute washes with PBS. After adding 1 mL of β-galactosidase staining solution (Sigma, USA, #94433) to each well, Incubate in a 37 ℃ constant-temperature box for 12 h. Aspirate the staining solution, add PBS, and ob-serve the cell staining under a microscope. Non-senescent cells show no obvious blue col-or, while senescent cells appear blue. Calculate the percentage of blue-stained cells.

Tube formation assay

The 96-well plates were coated with 100 μL Matrigel (BD, USA, #356234). The 100 μL treated HUVECs (10^4 cells) were then added to each well. Tubular networks were imaged with a 5x objective lens after 6 h of incubation using a computer. ImageJ software was utilized to quantify tube length per field from the TIF images[14].

Western blot analysis

HUVECs were lysed in 150 μL of Beyotime buffer and thermally cracked for 7 min. The samples were then subjected to 10% SDS-PAGE and transferred onto PVDF membranes (Millipore Corp, MA, USA, #IPVH00010) via electrophoresis. Following blocking, membranes were incubated overnight at 4°C with primary antibodies: TP53 (CST, USA, #12282), AKT1 (Abcam, USA, #14179), p-AKT1 (Sigma, USA, #9441), PI3K (CST, USA, #9698), p-PI3K (Acam, USA, #3161) and β-Actin (Beyotime, USA, #8457). Membranes were incubated with secondary antibodies (Beyotime, China, #A0208) for 40 minutes, and bands were visualized using an ECL system (Millipore, CA, USA, #WBULS0500).

Statistical analysis

Results are presented as mean ± standard deviation (SD), with statistical analysis performed using the Student's t-test and ANOVA. A p-value below 0.05 was deemed statistically significant.

Results

Potential action targets of SDF in treating aging

Protein targets for SDF were collected from the 6 databases. Following the removal of duplicate targets, 88 relevant SDF targets were identified, as depicted in Fig. 2A. Aging-related targets were identified using the 5 databases. After removing duplicates, 741 targets were identified, as shown in Fig. 2B. The GEO identified 9789 aging-related targets, illustrated in a volcano plot in Fig. 2C. Figure 2D illustrates the compilation of 102 intersection targets between SDF and aging.

Construction of PPI and selection of core targets

The STRING platform was used to input the intersection targets of SDF and aging, setting the interaction score to 0.8. This process generated a PPI network graph comprising 124 nodes and 498 edges, depicting the interactions among protein targets. The larger nodes indicate the most crucial protein targets. In Fig. 3, TP53, AKT1, TNF, ESR1 and IL6 are the top 5 targets, with degree values of 42, 29, 26, 24 and 22, respectively. Subsequently, TP53 were recognized as key targets for SDF in addressing aging and underwent molecular docking with SDF (Fig. 3).

Molecular docking

Molecular docking was conducted using Autodock Vina to analyze interactions between the core target protein TP53 and the 5 primary active ingredients of SDFE: quercetin, genistein, luteolin, kaempferol, and isorhamnetin, utilizing their 3D structures. Binding energies under − 5 kcal/mol indicate a strong level of affinity between large and small molecules. The compounds quercetin, genistein, luteolin and isorhamnetin demonstrated significant binding energies of − 4.9, − 5.18, − 7.24, − 5.13, and − 5.73 kcal/mol, respectively. Consequently, the docking interactions between these compounds and TP53 were further analyzed and visualized. According to the 3D diagrams in Fig. 4, core compounds primarily bind to TP53 via traditional hydrogen bonds and π- π stacking interactions. Similar to hydrogen bonds, π-π stacking is a form of noncovalent interaction and is considered a weak bond. Their weak bonding stabilizes protein-ligand binding at a certain level while facilitating its breakdown. As a result, they are essential in controlling the protein-ligand binding process, ensuring drugs are both effective and safe.

Construction of protein GO and KEGG network

Figure 5 presents the protein-GO-KEGG network, consisting of 287 nodes and 1254 edges. The GO and KEGG pathways share 182 intersection genes. The graph demonstrates that SDF influences multiple targets in aging therapy, causing a range of biological effects and mechanisms. Among the intersecting genes, the proteins exhibiting the highest degree values are CASP3, BCL2, IL6, AKT1, IL-1β, TNF, MAPK1, MMP2, EGFR, TP53 and MDM2. Notabe primary targets identified in the PPI network.

β-galactosidase staining

Figure 6 demonstrates that the model groups had a notably lower positive rate of aging HUVECs than the control group, suggesting that SDFE can counteract H2O2-induced aging of HUVECs.

Tube formation assay

The effect of SDFE on cellular aging was detected phenotypically. The tube-forming ability of HUVECs was assessed following the addition of SDFE.It was found that tube-forming ability was enhanced upon addition of SDFE, indicating that SDFE can protect HUVECs from aging (Fig. 7).

Western blot analysis

Protein expression levels in HUVECs were assessed by Western blot after SDFE was added. The p53 pathway linked to cellular aging was notably diminished in all SDFE dose groups compared to the control group. The p-Akt/Akt and p-PI3K/PI3K levels decreased significantly in all SDFE dose groups compared to the control group, exhibiting a dose-dependent pattern (Fig. 8).

Discussion

Using network pharmacological analysis, this study identified the key targets and pathways underlying SDF's anti-aging effect. Based on network pharmacology results, the main active components are quercetin, genistein, luteolin, kaempferol and isorhamnetin. The database and related software superimposed aging-related genes with potential SDF targets, and a total of 81 potential SDF anti-aging targets were identified. Through the PPI network for gene cross-filtering, the top 5 key factors with the most associated effects in the network were identified: TP53, AKT1, TNF, ESR1, and IL6. TP53, a key regulator of cell apoptosis, is significantly associated with cancer, aging, and cardiovascular diseases[15].

The promoter region of the PTEN gene can be directly bound by TP53, thereby promoting its transcription. PTEN is a lipid phosphatase that can reverse-convert PIP3, a product of PI3K, to PIP2, thereby directly terminating the transmission of PI3K/AKT[16]. Therefore, decreased TP53 expression may lead to increased PI3K/AKT expression. The PI3K/Akt pathway is a crucial intracellular signaling mechanism. It is essential in numerous physiological and pathological processes, including cell proliferation, survival, differentiation, growth and apoptosis [17]. ZHANG Y et al.[18] found that activating the PI3K/Akt/Nrf2 pathway could improve behavioral disorders and neurological deficits in aging mouse models. Our findings indicated that SDF enhances the protein expression levels of p-PI3K/PI3K and p-AKT/AKT. It suggests that SDF can delay the aging process of HUVECs through the TP53-PI3K/Akt pathway. The study offers new perspectives on aging, and further research will delve into the mechanisms by which SDFE affects HUVECs and the TP53-PI3K/Akt pathway.

Data availability

All data were included in this manuscript and could be obtained from the corresponding authors via email.

Declarations

Competing interests

The authors declare that the research was conducted in the absence of any commercial or financial relationships that could be construed as a potential conflict of interest.

Funding

This research was funded by the Doctoral Research Startup Fund of Guizhou University of Traditional Chinese Medicine (grant number 2022[15]), the Guizhou Provincial Department of Education Key Research Base of Humanities and Social Sciences (grant number 23RWJD158) and the Guizhou Science and Technology Department (grant number [2019]1019).

Author Contribution

BD. conducted the experiments, Z.-G.J., A.-X.S.and C.-G.H. conducted data processing and statistical analysis.S.L., Z.-R.X.and Y.-Y.Y. designed the experiments and edited the manuscript.

Data Availability

All data were included in this manuscript and could be obtained from the corresponding authors via email.

References

1. Schmeer, C., Kretz, A., Wengerodt, D., Stojiljkovic, M. & Witte, O. W. Dissecting Aging and Senescence-Current Concepts and Open Lessons. *Cells* **8** 10.3390/cells8111446 (2019).
2. Moskalev, A. et al. Targeting aging mechanisms: pharmacological perspectives. *Trends Endocrinol. Metab.* **33**, 266–280. 10.1016/j.tem.2022.01.007 (2022).
3. López-Otin, C., Blasco, M. A., Partridge, L., Serrano, M. & Kroemer, G. Hallmarks of aging: An expanding universe. *Cell* **186**, 243–278. 10.1016/j.cell.2022.11.001 (2023).
4. Cheng, M. et al. AGEs induce endothelial cells senescence and endothelial barrier dysfunction via miR-1-3p/MLCK signaling pathways. *Gene* **851** 10.1016/j.gene.2022.147030 (2023).
5. Du, X. H. et al. Anti-Aging of the Nervous System and Related Neurodegenerative Diseases With Chinese Herbal Medicine. *Am. J. Alzheimers Disease Other Dementias*. **38** 10.1177/15333175231205445 (2023).
6. Zhang, Z. J. et al. Unusual matrine-adenine hybrids isolated from Sophora davidii and their inhibitory effects on human cytomegalovirus. *Phytochemistry* **190** 10.1016/j.phytochem.2021.112842 (2021).

7. Song, P. et al. Davidones F and G, Two Novel Flavonoids from Sophora davidii (Franch.) Skeels. *Molecules (Basel Switzerland)*. **26** 10.3390/molecules26144182 (2021).
8. Yang, P. F., Yang, J., Huang, S., Wei, T. & Mao, D. B. CHEMICAL CONSTITUENTS OF THE FLOWERS OF Sophora davidii. *Chem. Nat. Compd.* **56**, 948–950. 10.1007/s10600-020-03196-8 (2020).
9. Zhu, Y., Wang, Z., Gao, C., Zhang, L. & Sui, R. B. Oxymatrine-mediated prevention of amyloid β-peptide-induced apoptosis on Alzheimer's model PC12 cells: in vitro cell culture studies and in vivo cognitive assessment in rats. *Inflammopharmacology* **31**, 2685–2699. 10.1007/s10787-023-01291-0 (2023).
10. Sun, K. Y., Yang, P. Y., Zhao, R., Bai, Y. T. & Guo, Z. J. Matrine Attenuates D-Galactose-Induced Aging-Related Behavior in Mice via Inhibition of Cellular Senescence an Oxidative Stress. *Oxid. Med. Cell. Longev.* (2018). 10.1155/2018/7108604 (2018).
11. Kanehisa, M., Sato, Y., Kawashima, M., Furumichi, M. & Tanabe, M. KEGG as a reference resource for gene and protein annotation. *Nucleic Acids Res.* **44**, D457–462. 10.1093/nar/gkv1070 (2016).
12. Ogata, H. et al. Kyoto Encyclopedia of Genes and Genomes. *Nucleic Acids Res.* **27**, 29–34. 10.1093/nar/27.1.29 (1999).
13. Chen, P. et al. Investigating mechanisms of Sophora davidii (Franch.) skeels flower extract in treating LPS-induced acute pneumonia based on network pharmacology. *J. Ethnopharmacol.* **337** 10.1016/j.jep.2024.118914 (2025).
14. Zudaire, E., Gambardella, L., Kurcz, C. & Vermeren, S. A Computational Tool for Quantitative Analysis of Vascular Networks. *PLoS One*. **6** 10.1371/journal.pone.0027385 (2011).
15. Chappell, W. H. et al. Influences of TP53 and the anti-aging DDR1 receptor in controlling Raf/MEK/ERK and PI3K/Akt expression and chemotherapeutic drug sensitivity in prostate cancer cell lines. *Aging-Us* **12**, 10194–10210. 10.18632/aging.103377 (2020).
16. Chen, H., Deng, J., Hou, T. W. & Shan, Y. Q. Villosol reverses 5-FU resistance in colorectal cancer by inhibiting the CDKN2A gene regulated TP53-PI3K/Akt signaling axis. *J. Ethnopharmacol.* **325** 10.1016/j.jep.2024.117907 (2024).
17. Yuan, F. H. et al. Molecular Mechanisms of Lobelia nummularia Extract in Breast Cancer: Targeting EGFR/TP53 and PI3K-AKT-mTOR Signaling via ROS-Mediated Apoptosis. *Curr. Issues Mol. Biol.* **47** 10.3390/cimb47070546 (2025).
18. Zhang, Y. et al. Naringenin Ameliorates Behavioral Dysfunction and Neurological Deficits in a d-Galactose-Induced Aging Mouse Model Through Activation of PI3K/Akt/Nrf2 Pathway. *Rejuven. Res.* **20**, 462–472. 10.1089/rej.2017.1960 (2017).

Figures



Figure 1

Sophora davidii flower and related dishes. (A) Sophora davidii flower. (B) Pancake made from Sophora davidii flower.

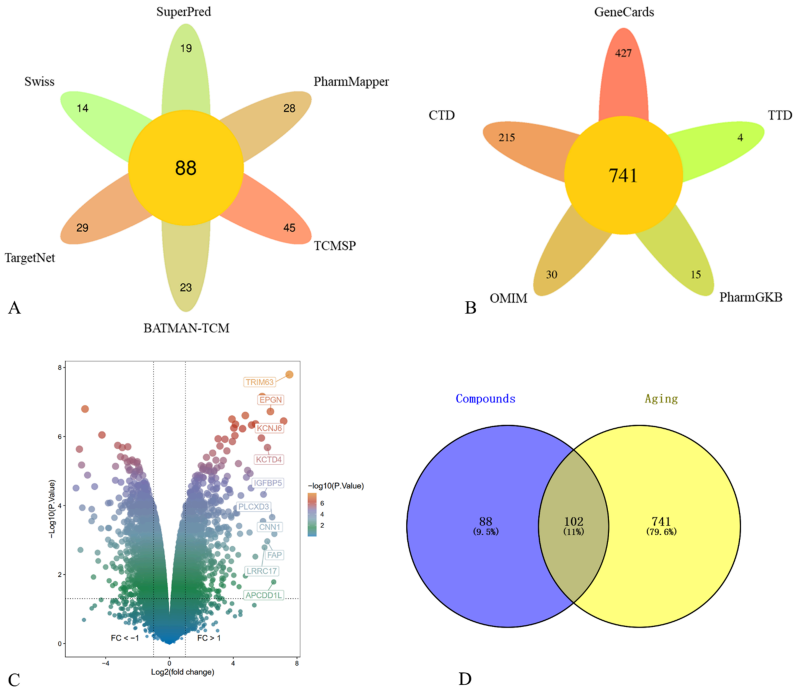


Figure 2

Targets of SDF or/and Aging. (A) SDF targets in six open-source databases; (B) Targets of Aging in five open-source databases; (C) Volcano diagram of targets of aging; (D) The intersection of SDF and Aging.

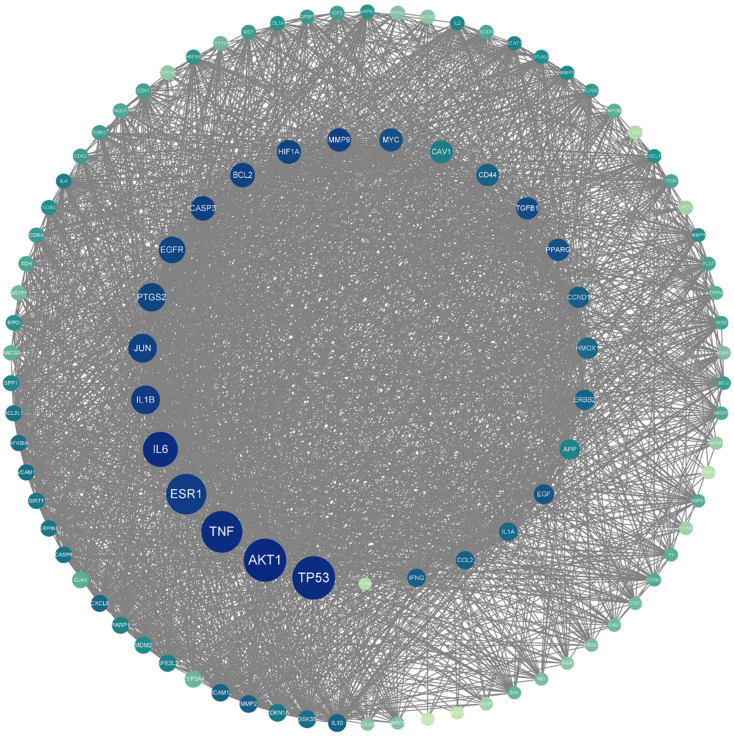


Figure 3

Protein–protein interaction network graph of intersection genes

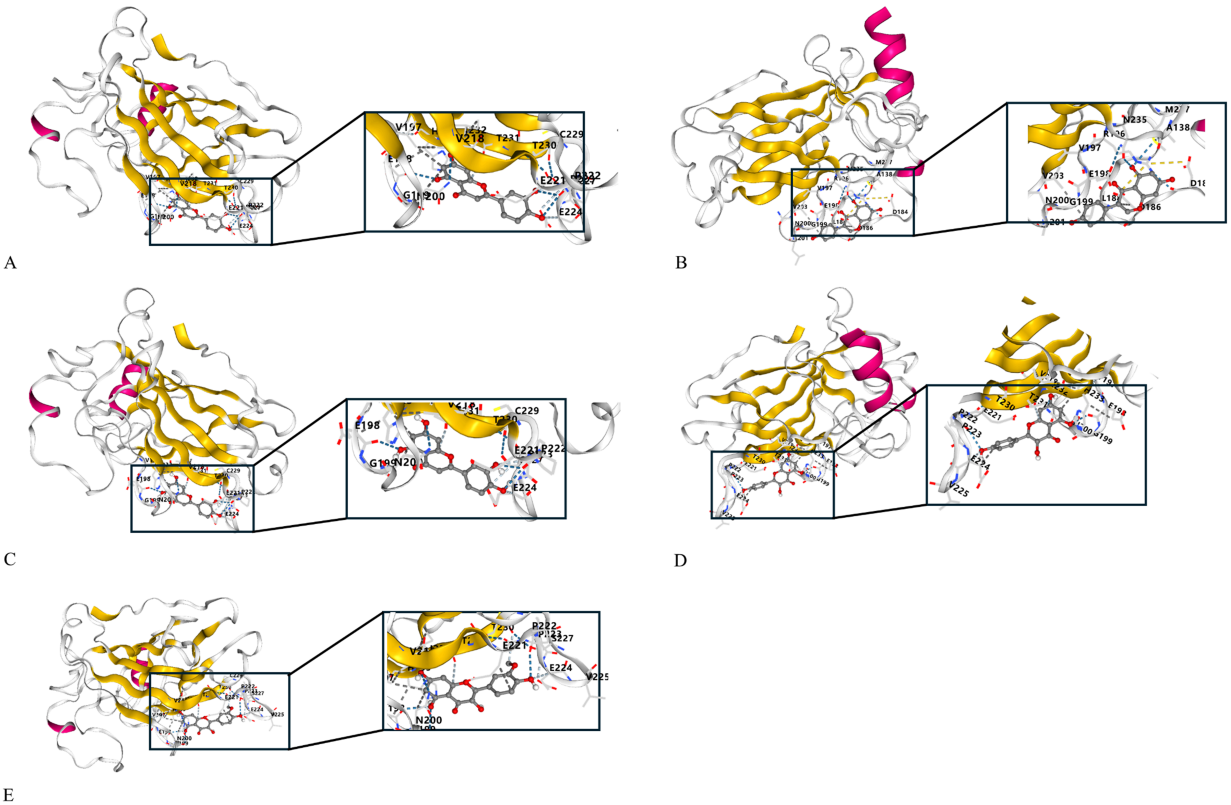


Figure 4

Schematic diagram of docking between active compounds and TP53. (A–E) represent the molecular binding of TP53 with quercetin, genistein, luteolin, kaempferol and isorhamnetin, respectively.

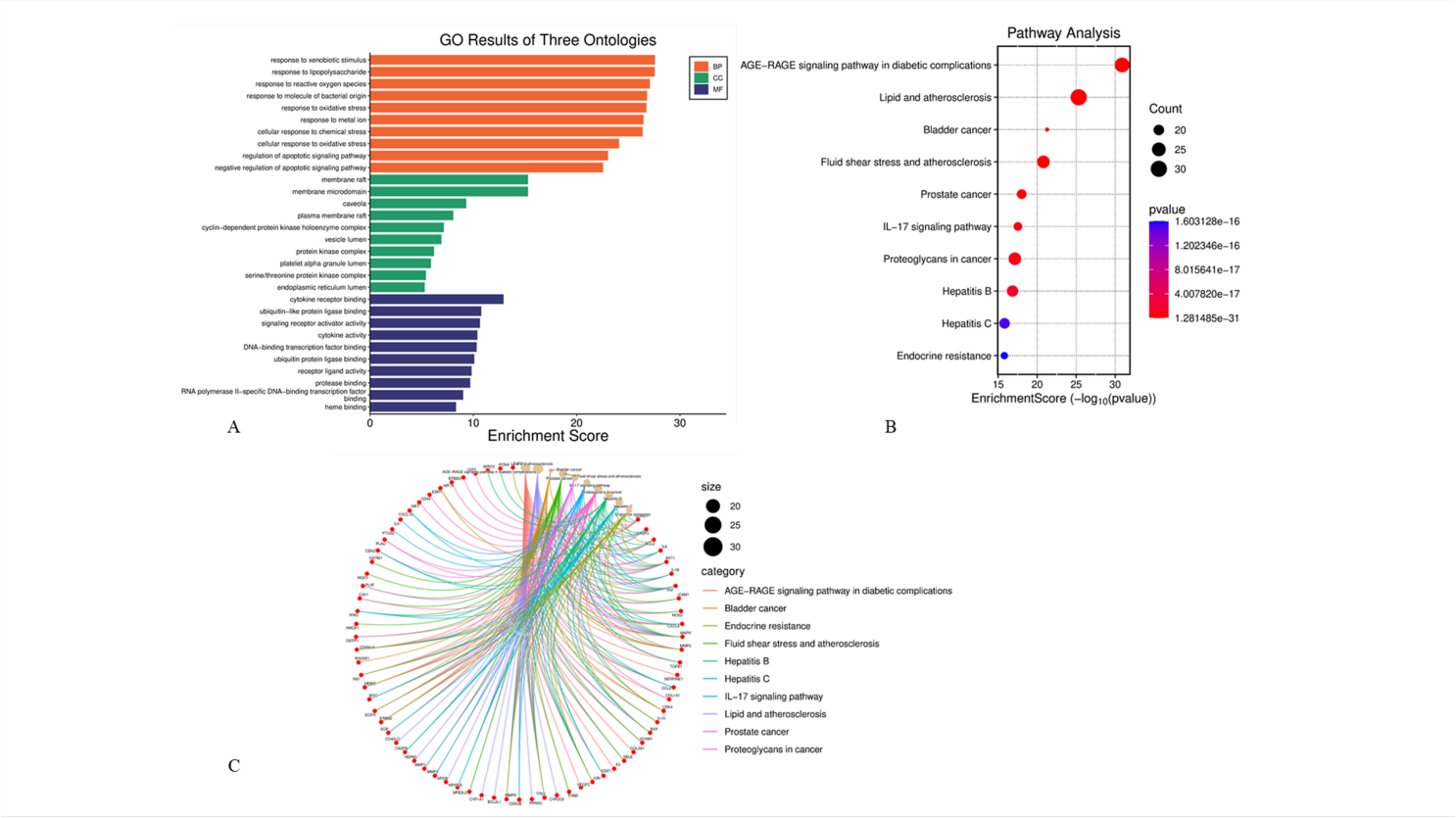


Figure 5

Gene Ontology (GO) and Kyoto Encyclopedia of Genes and Genomes (KEGG) analysis of intersection genes between SDF and Aging. (A) GO analysis. (B) KEGG analysis. (C) KEGG circle diagram.

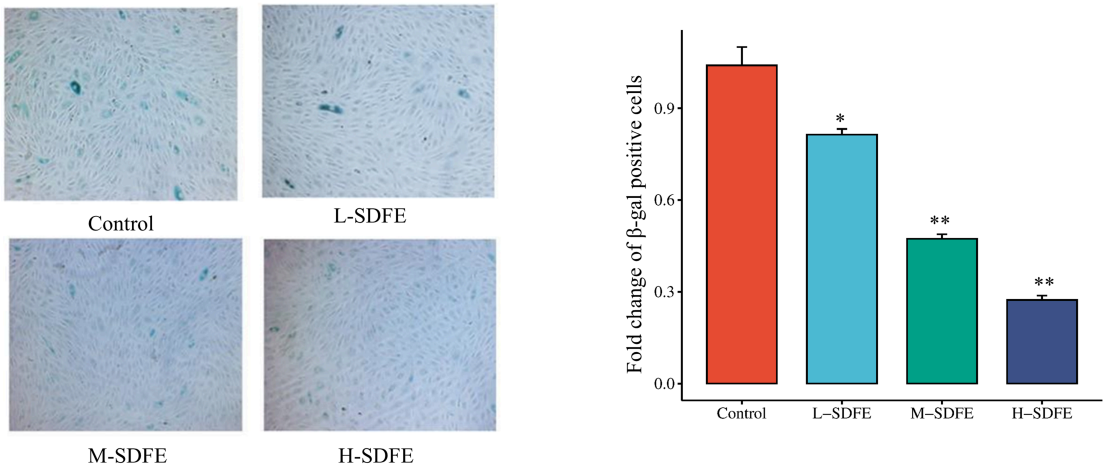


Figure 6

β-galactosidase staining was used to detect the effect of SDFE on the Aging of HUVECs. The data were presented as the means ± SD; n = 3; *$p < 0.05$, **$p < 0.01$.

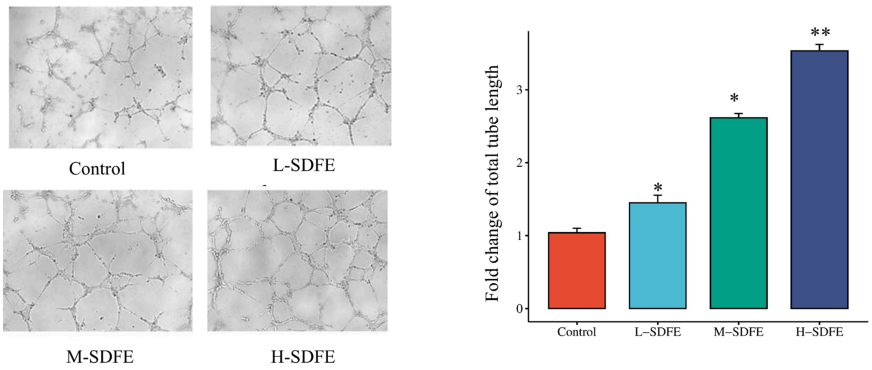


Figure 7

The effect of SDFE on the tubation ability of HUVECs. The data were presented as the means ± SD; n = 3; *$p < 0.05$, **$p < 0.01$,

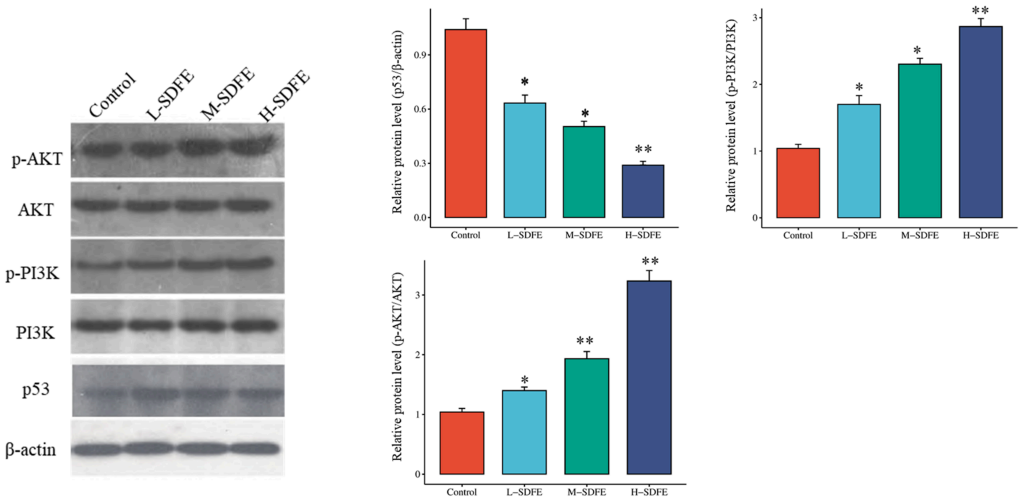


Figure 8

The influence of SDFE on the key protein expression levels in HUVECs. The data were presented as the means ± SD; n = 3; *$p < 0.05$, **$p < 0.01$.

Supplementary Files

This is a list of supplementary files associated with this preprint. Click to download.

- KEGGPERMISSION261296.pdf
- OriginalImagesforBlots2.pdf
- permission.pdf
- Voucherspecimen.pdf